

NRC Publications Archive Archives des publications du CNRC

Measurement of transmissivity in outdoor soot plumes using sky-scattered solar radiation

Yang, C.; Thomson, Kevin; Johnson, M.

This publication could be one of several versions: author's original, accepted manuscript or the publisher's version. /
La version de cette publication peut être l'une des suivantes : la version prépublication de l'auteur, la version acceptée du manuscrit ou la version de l'éditeur.

Publisher's version / Version de l'éditeur:

*Combustion Institute Canadian Section, 2008 Spring Technical Meeting
[Proceedings], 2008*

NRC Publications Archive Record / Notice des Archives des publications du CNRC :

<https://nrc-publications.canada.ca/eng/view/object/?id=d63d1a5f-46e3-4aca-8859-66e7331f24be>
<https://publications-cnrc.canada.ca/fra/voir/objet/?id=d63d1a5f-46e3-4aca-8859-66e7331f24be>

Access and use of this website and the material on it are subject to the Terms and Conditions set forth at
<https://nrc-publications.canada.ca/eng/copyright>

READ THESE TERMS AND CONDITIONS CAREFULLY BEFORE USING THIS WEBSITE.

L'accès à ce site Web et l'utilisation de son contenu sont assujettis aux conditions présentées dans le site
<https://publications-cnrc.canada.ca/fra/droits>

LISEZ CES CONDITIONS ATTENTIVEMENT AVANT D'UTILISER CE SITE WEB.

Questions? Contact the NRC Publications Archive team at
PublicationsArchive-ArchivesPublications@nrc-cnrc.gc.ca. If you wish to email the authors directly, please see the first page of the publication for their contact information.

Vous avez des questions? Nous pouvons vous aider. Pour communiquer directement avec un auteur, consultez la première page de la revue dans laquelle son article a été publié afin de trouver ses coordonnées. Si vous n'arrivez pas à les repérer, communiquez avec nous à PublicationsArchive-ArchivesPublications@nrc-cnrc.gc.ca.

Measurement of transmissivity in outdoor soot plumes using sky-scattered solar radiation

C. Yang^a, K.A. Thomson^b, M.R. Johnson^{a*}

^a *Mechanical and Aerospace Engineering, Carleton University, Ottawa, Canada*

^b *Combustion Group, Institute for Chemical Process & Environmental Tech., NRC*

1. Introduction

Currently there is a lack of practical approaches for quantifying soot emission rates from unconfined industrial sources such as stack plumes and flares. Most regulatory standards are based on a human-observed opacity standard as outlined in U.S. Environmental Protection Agency Method 9 [1]. This paper is the third part of an investigation of a sky-scattered solar radiation based optical diagnostic for plume transmissivity measurement. The technique is based on the established laboratory optical technique known as diffuse Two Dimensional Line-of-sight attenuation (2D-LOSA) [2, 3], in which images of a light source, the light source through a plume, and plume alone are compared in a so-called “3-image” algorithm. However, when the technique is transferred to an outdoor setting where the light source is sky-scattered solar radiation, a “1-image” algorithm must be used, in which the unattenuated light in the plume region must be interpolated from other regions of the image. A detailed explanation of 2D-LOSA 3-image vs. 1-image routines for lab and outdoor measurements can be found in previous papers [4, 5]. This paper is focused on 1) background interpolation analysis under different sky conditions to determine unattenuated intensities behind the plume; 2) comparison of measurements of soot in an unconfined plume using both lab-based and sky-LOSA techniques; and 3) determination of the ultimate accuracy and sensitivity limits in terms of soot emission rate for the sky-LOSA technique.

2. Methodology

A stable plume of soot was generated using an inverted methane/air co-annular non-premixed burner modified by Coderre *et al* [6] following a similar design developed by Stipe *et al.* [7]. The combustion products mixed with excess air flowed through a 15.9 mm diameter, 140 cm long U-shaped tube in which they cooled before exiting through a smooth converging nozzle to create an unconfined, vertical soot plume. For some conditions, a secondary dilution air stream was also injected just downstream of the tip of the flame to enhance dilution and cooling of the combustion products. The soot concentration in the plume could be controlled by adjusting the relative amounts of fuel, co-flow air, and secondary dilution air. Table 1 lists conditions for the different tests that were evaluated in this study. The transmissivity values corresponding to each test were obtained from in-lab diffuse-LOSA measurements. The table also shows that the air flow rates (from 14.5 SLPM to 16 SLPM) are more than 12 times the stoichiometric requirement for the fixed fuel flow studied (1200 SCCM), i.e., all flames were greatly over ventilated.

LOSA measurements of optical transmissivities through the soot plume of the inverted flame burner were obtained indoors under lab-conditions using diffuse-light from an arc-lamp and outdoors using sky-scattered solar radiation. By applying the Rayleigh-Debye-Gans scattering approximation in which soot

* Corresponding Author: Matthew_Johnson@carleton.ca

aggregates are treated as polydisperse fractal aggregates, and using the Beer-Lambert-Bouguer Law, experimentally measured optical transmissivities through a soot-containing sample volume are transformed into soot volume fraction data (cf. [8]). The mass emission rate of soot from plumes is functionally related to plume transmissivity as specified in Eq. (1) [9].

$$\dot{m}_{\text{soot}} = \frac{-u\rho_{\text{soot}}\lambda}{6\pi E(m)_{\lambda}(1+\rho_{\text{sa},\lambda})} \int \ln(\tau_{\lambda}(y))dy \quad (1)$$

where \dot{m}_{soot} is mass emission rate of soot; u is plume velocity, ρ_{soot} is soot density and taken to be 1.8-1.9 g/mL as used by Flower and Bowman [10]; λ is wavelength of the transmissivity measurement and equals 577 nm in the experiment; $E(m)_{\lambda}$ is a wavelength dependent refractive index function for soot and equals 0.258 as used by Snelling [2]; $\rho_{\text{sa},\lambda}$ is the wavelength dependent ratio of scatter to absorption for the light traveling along a chord through the plume and varies from 0.2-0.4 for overfire soot from a variety of fuels in turbulent diffusion flames as determined by Kooyu and Faeth [11]; and τ_{λ} is plume transmissivity measured normal to the plume propagation direction.

Table 1 Burner operating conditions corresponding to the plume transmissivities

| Test Conditions | CH4 flow rate [SCCM] | Co-flow air flow rate [SLPM] | Dilution air flow rate [SLPM] | Plume transmissivity |
|-----------------|----------------------|------------------------------|-------------------------------|----------------------|
| Test 1 | 1200 | 14.5 | 10 | 0.974 |
| Test 2 | 1200 | 15 | 20 | 0.982 |
| Test 3 | 1200 | 15.5 | 30 | 0.986 |
| Test 4 | 1200 | 15.5 | 60 | 0.991 |
| Test 5 | 1200 | 16 | 70 | 0.994 |
| Test 6 | 1200 | 16 | 90 | 0.995 |

3. Results and Discussion

3.1 Background Interpolation Analysis

In the field application of 2D LOSA, using sky-scattered solar radiation as the light source, it is impossible to isolate the background from the attenuating medium. Therefore, an interpolated background must be generated from a single “transmission image” to allow calculation of the plume transmissivity in a process known as the 1-image method. To generate the *interpolated background*, the section of an image is removed where a plume is present and the intensity data on either side of the plume image location is used to interpolate a synthetic background in the region of the plume. Interpolation was performed using a Mathcad implementation of the Loess algorithm which relies on a locally weighted least square method to fit local quadratic profiles to measured intensity data. The background interpolation error depends on the choice of two parameters: the value of *span* argument of Loess function and the width of plume in the image (also called the plume size). The span argument is defined as the fraction of total number of data points included in the local fit. The importance of each these points is weighted by their distance from the interpolation point in a cubic function. The plume size is defined here to be the plume width in the image relative to the total image width.

To develop guidelines for the uncertainty introduced by different possible sky conditions during field measurements, thirty (30) sky images were collected for each of clear, cloudy, and overcast sky conditions. Figure 1a shows reference photographs of the sky under each of the three conditions. For each image, five (5) different theoretical plume sizes were evaluated by interpolating and comparing intensities for the center 10%, 20%, 30%, 40%, or 50% of the image width. For each of these theoretical plume sizes, thirteen (13) different values of *span* were tested from 0.1 to 0.7 with an increment of 0.05. It was found that the effect of changing the *span* values in the Loess interpolation produced insignificant change in the

interpolation bias for various sky conditions relative to the effect of varied plume size in the image. As expected, the interpolation uncertainties increase with increasing the plume width in the image. Therefore, it is important to set guidelines for plume size in the transmission measurements.

By comparing interpolated intensities in the sky images with actual measured intensities, the background interpolation biases for various sky conditions with respect to different plume sizes were calculated as an uncertainty or bias in transmissivity. The apparent sky transmissivity is defined as $\tau_{sky} = I_{sky,fit} / I_{sky,measured}$, where $I_{sky,fit}$ is the interpolated sky intensity generated using the Loess fit function and $I_{sky,measured}$ is the actual measured intensity data. Ideally, the transmissivity would be unity. The bias introduced by the interpolated sky transmissivity is quantified by integrating $\ln(\tau_{sky})$ over the interpolated region and dividing by that width, as is plotted in Figure 1b.

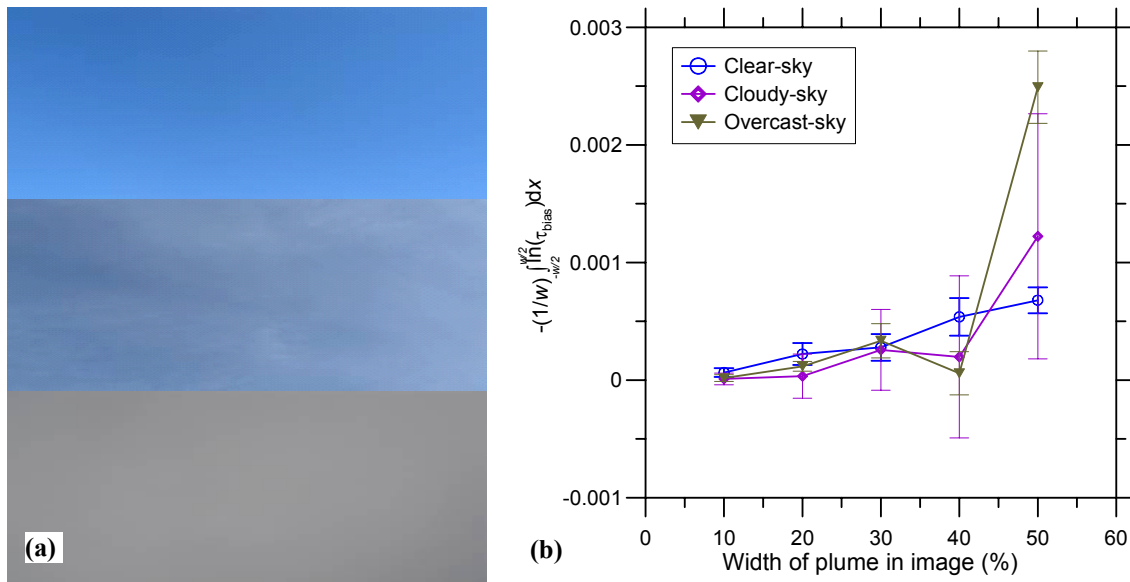


Figure 1 a) Clear, Cloudy, and Overcast sky conditions b) Background interpolation bias under these conditions.

Data points in the figures are calculated means of 30 individual measurements with the error bars indicating 95% confidence intervals of the means ($\pm 2\sigma$). Comparing various sky conditions, the interpolation bias and the measurement uncertainties under clear sky condition are the lowest. The measurement uncertainties are highest for the cloudy sky condition. Therefore, a clear sky condition is preferred for plume transmissivity measurements in the field. However, measurements appear possible for any condition, in particular if the width of the plume in the image remains small. Curiously, the mean bias errors in Figure 1b are all greater than zero. This bias was shown to be statistically significant through a null hypothesis analysis using Student t-test statistics and is attributable to the interpolation algorithm.

Figure 1b also shows the importance of plume width in the image. Considering both the mean biases and their uncertainties, it is recommended that the plume width be less than 30% of the image width. Since optimization of the span setting for Loess interpolation depends on weather conditions, it is not possible to provide a single guideline for all situations. However, in a practical application of the sky-LOSA technique to measure plumes outdoors, it would be possible to take sky images just before or after actual plume measurements so that an analysis similar to the one described here could be performed to choose optimal parameters for the Loess interpolation algorithm on a case-by-case basis.

It is evident that interpolation can lead to uncertainty in the measurement. This bias should be no larger than the mean bias as indicated in Figure 1b plus two times the uncertainty of that mean bias. For the data collected for the three sky conditions presented here, and assuming a 30% plume size, the biases are 3.93×10^{-4} , 8.87×10^{-4} , and 4.81×10^{-4} for clear, cloudy, and overcast sky conditions, respectively. Assuming nominal environmental conditions of 12.5 km/h plume velocity and 2 m plume width, the associated errors in soot emission rates contributed by the background interpolation bias are estimated based on Eq. 1 to be 0.49 mg/s, 1.1 mg/s, and 0.59 mg/s for clear, cloudy, and overcast sky conditions, respectively. Compared to an estimated nominal soot emission rate from solution gas flares of 4.24 mg/s [9], these biases represent uncertainties of 11, 26, and 14% respectively.

3.2 Turbulent Plume Measurement

Plume transmissivity measurements were performed using the soot plume generated from the inverted-flame burner and sky-scattered solar radiation as the illumination source. Experiments were conducted to directly compare results of outdoor sky-scattered solar radiation measurements with in-lab diffuse-LOSA measurements for the same test conditions. The ultimate accuracy and sensitivity limits of the sky-LOSA approach were investigated. Six (6) test conditions were evaluated in this study, corresponding to transmissivity values from 0.974 to 0.995 obtained from in-lab diffuse LOSA. The experiments were repeated under different sky conditions.

To simplify the sky-LOSA measurements, experiments were conducted in a large garage area so that the majority of the experimental hardware could be sheltered in the garage and in particular, the environmental conditions of the burner could be better controlled to match those of the in-lab diffuse-LOSA measurements. During the experiments, the large garage door was fully opened, and a large (1 m by 0.76 m) flat mirror was positioned just outside the lab and aligned with the burner tip and the camera, to reflect sky light through the plume and into the camera system. A black screen was also placed outside to prevent the sun from directly shining onto the system. The detector was positioned relative to the center plan of the burner exhaust nozzle so that the plume width was less than 25% of the image width after allowing for some plume movement due to the wind effects.

Statistical analysis of measurements of sky intensities with and without the mirror and interpolation bias analysis similar to that described above, revealed that the presence of the mirror had negligible influence on results. However, as tests were performed in winter, the lab temperature did drop significantly when the garage door was opened for sky-LOSA measurements, which could have influenced the temperature at the burner exit nozzle leading to a difference between diffuse LOSA and sky LOSA for the same test conditions.

Experimental data were collected by taking thirty (30) plume attenuating images for each test condition using both in-lab diffuse light and sky light under clear-sky, cloudy-sky, and overcast-sky condition. For the diffuse-LOSA measurements thirty (30) images were also taken of the light source without the plume present at each condition. A reference dark image of the camera was collected at the end of the each experiment. Plume transmissivities were calculated using the 3-image routine for diffuse LOSA and 1-image routine for sky LOSA measurements.

For the 1-image method, the background intensity was generated from the intensity data to the left and to the right of the plume using the Loess fit function. It should be noted that while generating the background intensity, the width of the plume for interpolation was determined 'by eye'. This was more critical for low light attenuating plumes and / or on windy days when the plume edges were not well-defined in the images. In the present experiments, the burner tip was 13.2% of the image width and plume sizes were estimated to be 15% to 22% of the image width depending on the amount of wind induced movement. Although it would be possible to use edge detection algorithms to automatically estimate the width of the plume, it was not obvious that these routines would improve results. Theoretically, overestimating the plume width would not alter the final results since transmissivities outside the plume should be unity. However, to minimize bias due to interpolation uncertainty, it would be preferable to avoid overestimation of the plume width as much as possible.

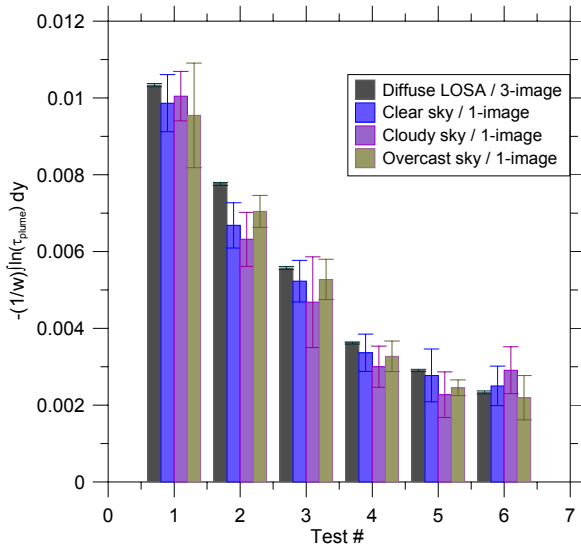


Figure 2 Comparison of 3-image diffuse LOSA applied to inverted flame in gray and 1-image sky LOSA under Clear-sky condition in blue, Cloudy-sky condition in pink, and Overcast-sky condition in green at the same test conditions.

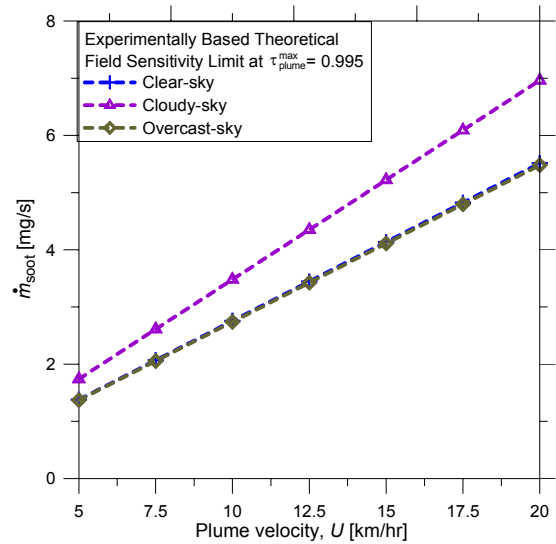


Figure 3 Theoretical detectable limits with sky-scattered light for field measurement conditions.

Figures 2 show comparison plots of $-(1/w)\int \ln(\tau_\lambda) dy$ values at equivalent test conditions for 3-image diffuse-LOSA measurements and 1-image sky-LOSA measurements under clear, cloudy, and overcast sky conditions. Data columns in Fig. 2 are the calculated means of 30 individual measurements with error bars indicating the 95% confidence intervals of the means ($\pm 2\sigma$). Overall, the 1-image sky light measurements agree well with the 3-image diffuse light measurements within experimental uncertainty. However, the mean $-(1/w)\int \ln(\tau_\lambda) dy$ values from sky-LOSA are consistently lower than reference values from 3-image diffuse LOSA measurements. Statistical testing revealed that this systematic bias was statistically significant, and is potentially attributable to the slight bias in background interpolation discussed above. Alternatively, it is possible that the differences in ambient temperature in the lab during diffuse-LOSA measurements and sky-LOSA measurements may have influenced the at the exhaust outlet of the burner and affected conditions in the plume. Future measurements, in warmer weather or where diffuse and sky LOSA measurements could be performed simultaneously would be beneficial.

In the present measurements, Test condition 6 represented the minimum soot loading that could be analyzed. This corresponds to a minimum transmissivity through the center of the plume of 0.995. Lower soot loadings were not attempted because it became impossible to observe the location of the plume, even though the background interpolation bias analysis suggests that higher minimum transmissivities should be possible. Figure 3 shows the minimum detectable mass flow rate of soot for a 2 m wide plume as a function of plume velocity, assuming a transmissivity limit of 0.995 from test condition 6 in Figure 2. Soot emission rates corresponding to the regions above the dashed lines are detectable for each sky condition. The detectable limits deteriorate (i.e. increase) as plume velocity increases. At a wind speed of 12.5 km/h (corresponding to a typical average wind speed for locations in Alberta), the theoretical minimum mass flow rate of soot that could be detected in a 2 m wide plume is 3.45 mg/s, 4.35 mg/s, and 3.43 mg/s for the clear-sky, cloudy-sky, and overcast-sky conditions, respectively. If we further assumed that the only uncertainty in the measurement is the interpolation uncertainty, the uncertainty on the measurement at the detectable limit as calculated above, would be 0.49 mg/s or 14%, 1.1 mg/s or 25%, and 0.59 mg/s or 17%. However, the interpolation uncertainties would be less significant for plumes with higher soot emission

rates corresponding to lower transmissivities. Certainly, other uncertainties do exist in the measurements and it is necessary to assimilate the present results into a total uncertainty analysis.

4. Conclusion

Experiments were performed to estimate limiting uncertainties in using sky-scattered solar radiation to measure transmissivity of soot laden plumes in an outdoor environment. The uncertainty associated with interpolating background intensities behind the plume depend strongly on the width of the plume in the image and weakly on the fit parameters when using Loess smoothing coupled with local polynomial interpolation. Based on the experimental results, a maximum plume width of 30% of the image width is a reasonable criterion for configuring image acquisition for plume transmissivity measurements. If the 3-image diffuse light technique is taken as a standard, with the current set-up, the highest plume transmissivity that could be measured in the field using the sky as the light source is 0.995. For 2 m diameter plume moving with a 12.5 km/h crosswind, the theoretical minimum mass flow rate of soot that can be detected is 3.45 mg/s, 4.35 mg/s, and 3.43 mg/s for clear, cloudy, and overcast sky conditions.

This is the first investigation to demonstrate 2D-LOSA in an outdoor application using sky-scattered solar radiation as the light source. The results suggest that the outdoor measurement technique is sufficiently accurate for industrial use and is likely to be a significant improvement over the existing methods.

Acknowledgments

This work has been financially supported by Environment Canada (Project Manager Michael Layer) and the Canadian Association of Petroleum Producers (CAPP).

References:

- [1] US EPA (1971) "Method 9 - Visual determination of the opacity of emissions from stationary sources," *Electronic Code of Federal Regulations*, 1971, pp. Title 40 - Protection of the Environment Part 60 - Standards of performance for new stationary sources - Appendix A-4, <http://www.epa.gov/ttn/emc/promgate/m-09.pdf>.
- [2] Thomson, KA, Johnson, MR, Snelling, DR, Smallwood, GJ, *Applied Optics*, 47(5):694-703 (2008)
- [3] Snelling, D. R, Thomson, K. A., Smallwood, G. J., Gulder, O. L., *Applied Optics*, 38:2478-2485 (1999).
- [4] C. Yang, K.A. Thomson, and M.R. Johnson (2006) Light Sources and Image Processing Methods for 2D Optical Transmissivity Measurements of Soot Plumes, Combustion Institute, Canadian Section, 2006 Spring Technical Meeting, Waterloo, ON, May 14-17, Paper N3, 6 pages.
- [5] C. Yang, K.A. Thomson, and M.R. Johnson (2007) Sensitivity limits in plume transmissivity measurements using sky scattered solar radiation, Combustion Institute, Canadian Section, 2007 Spring Technical Meeting, Banff, AB, May 13-16, Paper C2, 7 pages
- [6] A. Coderre, D.R. Snelling, G.J. Smallwood, and M.R. Johnson (2007) Measuring Optical Properties of Cooled Post-Flame Soot, Combustion Institute, Canadian Section, 2007 Spring Technical Meeting, Banff, AB, May 13-16, Paper E5, 6 pages.
- [7] Stipe, C.B., Higgins, B.S., Lucas, D., Koshland, C. P., & Sawyer, R.F. (2005). Inverted co-flow diffusion flame for producing soot. *Review of Scientific Instrument*, 76, 023908, 1-5
- [8] Sorensen, C.M. (2001) Light scattering by fractal aggregates: a review, *Aerosol Science & Technology*, 35:648-687.
- [9] Johnson, M.R. and Thomson K.A., Final report to Environment Canada, Mar. 2005.
- [10] Flowers, W.L. & Bowman, C.T., *Proc. Combust. Inst.*, 21:1115-1124 (1986).
- [11] Kooyul U.O., Faeth, G.M. *Transactions of the ASME*, 116: 152-159 (1994).